

1 Structural and Functional Characterization of Novel  
2 Phosphotyrosine Phosphatase Protein from *Drosophila*  
3 *Melanogaster* (Pupal Retina)

4  
5 Rubina Naz<sup>1</sup>, Anwar Iqbal<sup>2</sup>, Asma Saeed<sup>3</sup>, Alamzeb Khan<sup>4</sup>, Meshal Shutaywi<sup>5</sup>,  
6 Adriana Lavinia Cioca<sup>6</sup>, Narcisa Vrinceanu<sup>7\*</sup>

7 <sup>1</sup>Institute of Chemical Sciences, Gomal University, Dera Ismail Khan, Pakistan

8 <sup>2</sup>Department of Chemical Sciences, University of Lakki Marwat, Lakki Marwat,  
9 Pakistan.

10 <sup>3</sup> Center of Biochemistry and Biotechnology, Gomal University, Dera Ismail  
11 Khan, Pakistan.

12 <sup>4</sup> Department of Pediatrics, Yale School of Medicine, Yale University, New  
13 Haven, CT, 06511, USA.

14 <sup>5</sup> Department of Mathematics, College of Science & Arts, King Abdulaziz  
15 University, P.O. Box 344, Rabigh 21911, Saudi

16 <sup>6</sup>CMI Dr. Cioca Adriana-Lavinia, 22 Dorobantilor Street, Sibiu 557260, Romania.

17 <sup>7\*</sup> Faculty of Engineering, Department of Industrial Machines and Equipments,  
18 "Lucian Blaga" University of Sibiu, 10 Victoriei Boulevard, 550204, Sibiu,  
19 Romania.

20

21 Corresponding Author: Narcisa Vrinceanu

22 Address: Faculty of Engineering, Department of Industrial Machines and  
23 Equipment, "Lucian Blaga" University of Sibiu, 10 Victoriei Boulevard, 550204,  
24 Sibiu, Romania.

25 Contact: [vrinceanu.narcisai@ulbsibiu.ro](mailto:vrinceanu.narcisai@ulbsibiu.ro), Tel: +40 721428641

26

27

28

29

30

## 31 **Abstract**

32 A novel pair of protein Tyrosine Phosphatases in *Drosophila Melanogaster* (pupal  
33 retina) has been identified. Phosphotyrosyl protein phosphatases (PTPs) are  
34 structurally diverse enzymes increasingly recognized having fundamental role in  
35 cellular processes including effects on metabolism, cell proliferation and  
36 differentiation. This study presents comparative homology modeling of low  
37 molecular weight phosphotyrosine protein phosphatase (PTPs) from *Drosophila*  
38 *melanogaster* (Dr-PTPs) and their complexation with potent inhibitor HEPES. The  
39 3D structure was predicted based on sequence homology with bovine heart low  
40 molecular weight PTPs (Bh-PTPs). The sequence homology is approximately 50%  
41 identical to each other and to low molecular weight protein tyrosine  
42 phosphatases (PTPs) in other species. Comparison of the 3D structures of Bh-  
43 PTPs and Dr-PTPs (primo-2) reveals a remarkable similarity having a four  
44 stranded central parallel  $\beta$  sheet with flanking  $\alpha$  helices on both sides, showing  
45 two right-handed  $\beta$ - $\alpha$ - $\beta$  motifs. The inhibitor shows similar binding features as  
46 seen in other PTPs. The study also highlights the key catalytic residues important  
47 for target recognition and PTPs activation. The structure guided studies of both  
48 proteins clearly reveal a common mechanism of action, inhibitor binding at the  
49 active site and will expected to contribute towards the basic understanding of  
50 functional association of this enzyme with other molecules.

51

52 **Keywords:** PTPs; *Drosophila melanogaster*; homology modeling; sequence  
53 homology; enzyme substrate interactions;

54

## 55 **1. Introduction**

56 Low molecular weight phosphotyrosine protein phosphatases (PTPs), previously  
57 known as low molecular weight acid phosphatases, catalyzes the hydrolysis of  
58 tyrosine phosphorylated proteins, low molecular weight aryl phosphates and  
59 natural and synthetic acyl phosphates<sup>1,2</sup>. Although the activity of PTPs on serine  
60 and threonine phosphorylated proteins are very poor with the exception of flavin  
61 mononucleotide (FMN)<sup>3,4</sup>. Tyrosine phosphorylation plays a vital role in the  
62 regulation of the variety of developmental processes. These processes include  
63 several cell functions like growth, cell differentiation, metabolism, cell cycle and  
64 cyto-skeletal functions. Furthermore, the phosphorylation state of tyrosine and  
65 ser/thr of signaling proteins are controlled via specific reaction. Thus, the  
66 phosphorylation state is controlled by a very dynamic way to avoid severe  
67 malfunction of cell<sup>5</sup>.

68 PTPs can act as tumor suppressor by inhibiting cell growth. Functionally two  
69 types of PTPs sequences are conserved and well distinguished by structure  
70 comparison. The one known as classical PTPs are specific for tyrosine residues

71 and other with the dual-specificity phosphates (DSPS) are essential for serine and  
72 threonine dephosphorylation. The active site (C-(X)<sub>5</sub>-R) of these PTPs contains  
73 several conserved cysteine and arginine, important for catalyzing  
74 phosphorylation processes, and thus plays a vital role in regulation of signal  
75 transduction. All these acid phosphatase enzymes share little sequence  
76 homology, different range of molecular weight (18 kDa or above), but exhibit  
77 same catalytic mechanism <sup>6,7</sup>. The structural features of low molecular weight  
78 PTPs comprises relatively different fold comparing from fission yeast to  
79 mammals <sup>8,9</sup>. The overall three dimensional structural features contains four B  
80 sheets at center and surrounded by a helices <sup>6,10,11</sup>. However, several similarities  
81 can be seen in structural features and binding side pockets of PTPs to Mr-PTPs <sup>10-</sup>  
82 <sup>15</sup>. Importantly, the conserved the p-loop stabilized by complex hydrogen  
83 network and favor the phosphate trigonal bipyramidal transition state geometry  
84 <sup>16-19</sup>. Thus all low and higher Mr-PTPs and PTPs shares identical catalytic  
85 mechanism <sup>20</sup>. The enzymatic reaction is triggered by the first cysteine, where the  
86 substrate binding at active site is stabilized by the p-loop residues via hydrogen  
87 bonding and three anionic oxygen atoms. These transient interaction orient  
88 phosphorous atom in feasible position for nucleophilic attack and favors the  
89 enzymatic phosphorylation reaction <sup>20-22</sup>. The nucleophilic attack of thiol (S $\gamma$ )  
90 group takes place in the presence of proton donor aspartic acid and thus  
91 phosphor-cysteine intermediate is formed <sup>23-25</sup>. The formation of phosphor-  
92 cysteine intermediate is also favored and stabilized by the presence of p-loop  
93 where several residues are involved in binding and lowering the activation  
94 energy <sup>20</sup>. In the subsequent step, hydrolysis of phosphor-enzyme intermediate  
95 complex via attack of water takesplace, resulting in the liberation of inorganic  
96 phosphate (Pi). The enzymatic phosphorylation via hydrolysis works well at  
97 wide range of pH 5.5-7.5 from substrate.

98 The structural details of proteins are important parameters to understand the  
99 reactivity and stability of proteins. Several advance techniques like X-ray  
100 crystallography, nuclear magnetic resonance (NMR) and Electron Microscopy  
101 are frequently used to determine the structure of proteins. However, theoretical  
102 approaches like comparative modeling often used as a useful alternative to other  
103 biophysical and analytical techniques by providing insights into structural and  
104 functional aspects of proteins. In the current project, the comparative modeling  
105 technique has been used for the 3D structural prediction of sequence emerging  
106 from Primo-2 of *Drosophila melanogaster* (fruit fly) classified as low molecular  
107 weight PTPs family (LMW-PTPs). The present work is designed to elaborate the  
108 prediction of evolutionary context of the sequence homological ancestors,  
109 structural aspects and active site conformational states of *Drosophila Melanogaster*  
110 PTPs (Dr-PTPs) and spatial geometry formation of the active site. Dr-PTPs shares

111 46% amino acid sequence identity with that of Bh-PTPs (PDB: 1DG9) particularly  
 112 in active site regions.

## 113 2. Results and discussion

114

### 115 2.1. Sequence Analysis

116 Two novel pairs of proteins tyrosine phosphatases were identified in the  
 117 drosophila pupil retina. It was found that the primary sequences were  
 118 approximately 50% identical and characterized as low molecular weight protein  
 119 phosphatase (Fig. 1&2). The first sequence was incorporated at primo-1 (155  
 120 amino acid) and the other encoded by primo-2 (164 amino acid).

#### CLUSTAL X (1.81) MULTIPLE SEQUENCE ALIGNMENT

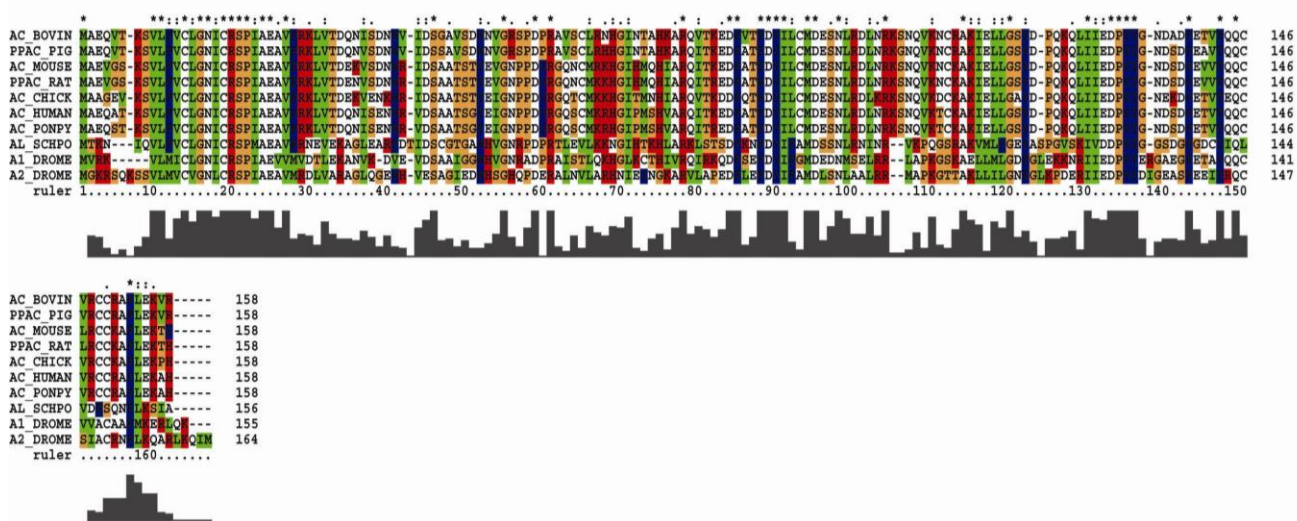


**Figure 1.** Multiple sequence alignment of 10 PTPs sequences. Sequences are named as Swiss-Prot entry first letter represents gene, the second part represents the biological source of gene. The symbol “\*” represents strongly conserved “.” represents weakly conserved “:” represents identical residues

121

122

```

                10         20         30         40         50         60
1DG9    AEQV-TKSVLFFVCLGNICRSPIAEAVFRKLVTDQNI SDNWVIDSGAVSDWNVGRSPDPRAVSCLRNHG
PTPs    GKRSQKSSVLMVCVGNLCRSPIAEAVMRDLVARAGLQGEWHVVE SAGIEDWHS GHQPDERALNVLARHN
                ***  *  *  *  *  *  *  *  *  *  *  *  *  *  *  *  *  *  *  *  *  *  *  *  *  *

                70         80         90         100        110        120        130
1DG9    INTAHKARQVTKEDFVTFDYILCMDESNLRLDINRKSNOVKNCRAKIELLGSYDPQ-KQLIEDPYYG-
PTPs    IEYNGKARVLAPEDFLEFDYIFAMDLSNLAALRRMAP--KGTTAKLLILGNFGLKPDERIIEDPYYDI
                *   ***   ***   ****   **  ***   *  *   *   **   **   **   *****

                140        150        160
1DG9    NDADFETVYQQCVRCCRAFLEKVR-----
PTPs    GEASFEEIYRQCSIACRNFLKQARLKQIM
                *  *  *  *  *  *  *  *  *  *

```

**Figure 2.** Pairwise sequence alignment used for building model of *Drosophila* phosphatase. Target sequence represented by PTPs. based on the structure of Bovin heart phosphatase template structure represented by 1DG9.

123

## 124 2.2. Structure Topology

125 The structure of Dr-PTPs (primo-2) comprises a fold containing four central  $\beta$   
 126 parallel sheets gathered by  $\alpha$ -helices: a right-handed  $\beta$ - $\alpha$ - $\beta$  motif. The conserved  
 127 sequence known as active site C—(X)<sub>5</sub>—R(S/T) of acid phosphatases was present  
 128 as sequence CVGNLCRS in Dr-PTPs. The active site was present in the form of  
 129 loop extending from between  $\beta$  1 and helix  $\alpha$ 1 (Fig. 4).

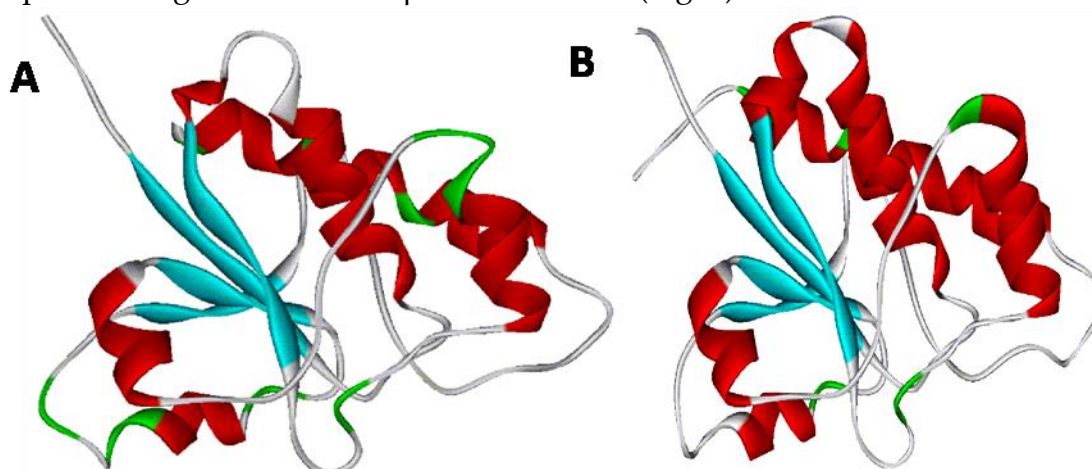


**Figure 3.** A complete Ribbon diagram of low molecular weight phosphotyrosine protein phosphatase. Showing  $\alpha/\beta$  Proteins,  $\alpha$  helix (Red),  $\beta$  Sheets (blue).(A) 1BVH(template), (B) *Drosophila*(target).

130

131 The crystal structure (PDB: IDG9) shows a complex of Bh-PTPs with HEPES,  
 132 where the active site residues were interacting with the sulfonate moiety,  
 133 accumulating phosphate binding manner in the pocket. All the oxygen atoms of

134 sulfonate group was involved in complex hydrogen bonding network, offered by  
135 N, H and S of the backbone residues of the active site loop and conserved  
136 arginine (Arg 18). The structural features of sulfonate complex were found  
137 similar to phosphates bounded at active sites. In our case, the highest sequence  
138 similarity of Dr-PTPs (Primo-2) primary sequence at substrate attracting site C-  
139 (X5)-R, tyrosine phosphorylation site RIIEDPYY was found. The 3D structure of  
140 Dr-PTPs (Primo-2) was superimposed at Bh-PTPs (Pdb: 1DG9). It was found the  
141 both structures aligned well for several motifs. However, regions like Gly 1, Lys  
142 6, Pro 105, Thr 108, Ile 134, Glu 136, Lys 121, Asp 123 and Leu 159, Met 163 of the  
143 Dr-PTPs structural orientation was different from the target. Furthermore, the  
144 sequence analysis on the basis of multiple sequence alignment and the  
145 construction of phylogenetic tree (PHYLP package) shows that both Dr-PTPs  
146 and Bh-PTPs belong to common ancestors. They are homologous sequences and  
147 members of same subfamily as per evolutionary context (Fig. 4).

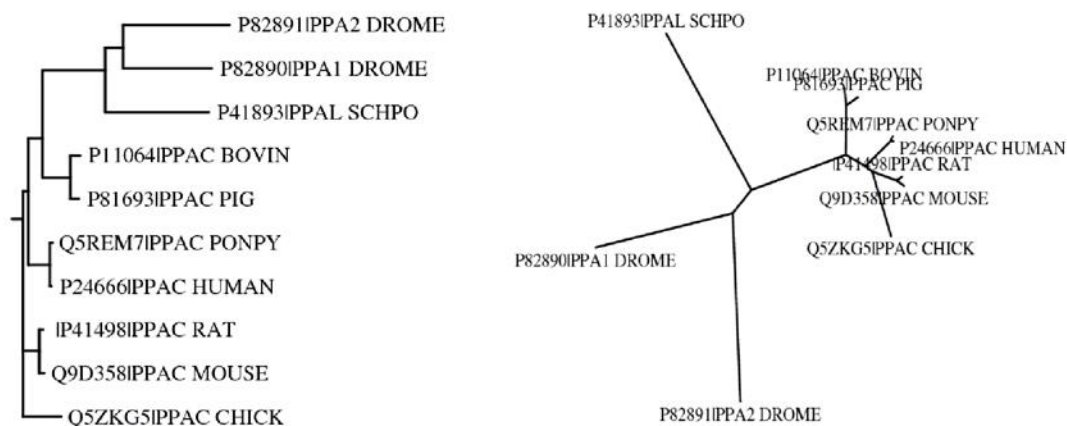


**Figure 4.** Dendrogram of PPA2 *Drosophila Melanogaster* and related proteins made by PHYLP & depicts relationship among various forms of PPAC,PPAI, PPA2 genes. The first part of the code represents gene where as the second part of the code represents the source of protein.

148

### 149 2.3. Structure Topology

150 The overall secondary and tertiary structure of the *Drosophila* phosphatase  
151 strongly resembles to templates 1BVH, 1DG9, 1PNT (Bovin heart) and other low  
152 molecular weight phosphotyrosine proteins phosphatase (Fig 3). The 3D  
153 structure was characterized with the active site end at the  $\alpha$ 1 and situated close  
154 to the N terminal region followed by the P-loop and  $\beta$ 1 strand. The active site  
155 emerged as deep groove encompassing aromatic residues ((Trp-49, Tyr-131, Tyr-  
156 132) appears like claws while the conserved residues Asp-56 and Arg 58 of  
157 variable loop provides a network of hydrogen bonds with other adjacent  $\alpha$ 5-  
158 helice and  $\beta$ 4-strand. All these residues work together for the target recognition

159 and sets a proper orientation of ligand for catalytically important residues Cys12,  
160 Cys17 and Arg18, whether Asp129 ( $\beta$ 4 extend loop) on the other end of the  
161 pocket to facilitate the protonation of phosphorylated intermediate together with  
162 Tyr131 and Tyr132. The hydrophobicity of active site groove is maintained by  
163 several buried hydrophobic residues like Leu 9, Val11, Phe82, Ile 88, Leu 99 and  
164 Lys 102.

#### 165 2.4. Quality of model

166 The different aspects of structure of Dr-PTPs were validated using  
167 different tools. The stereochemical outcomes were analyzed using software  
168 PROCHECK where the restraints obtained were compared to the stereochemical  
169 properties of Bh-PTPs. The degree of violation of secondary structure elements  
170 were evaluated using ramachandran plot where 94% regions were found in  
171 allowed region and no dihedral region in disallowed regions confirms the  
172 validity of the model.

173 The 10 best structures of the Dr-PTPs were compared with Bh-PTPs  
174 crystal structure, both in free and complexed with HEPES. The RMSD based on  
175 backbone ( $\alpha$ -carbon) were found 0.26 Å and 0.49 Å in the presence and absence  
176 of complexation (Table 1), respectively. These observations further confirmed the  
177 validity of the model beside the higher sequence identity. However, the  
178 conformational variability can be seen in several regions (1-6, 105-108, 134-136  
179 and 121-123) due to presence of different amino acids inducing different  
180 orientation (Fig. 7a).

181 **Table 1.**

Template	Target	DRMS
Bovin heart PTPs (1BVH) with out inhibitor	Drosophila PTPs	0.4840
Bovin heart PTPs (1DG9) with inhibitor (HEPES)	Drosophila PTPs	0.2549
Bovin heart PTPs (1PNT) with inhibitor (PO4)	Drosophila PTPs	0.1536

182

183

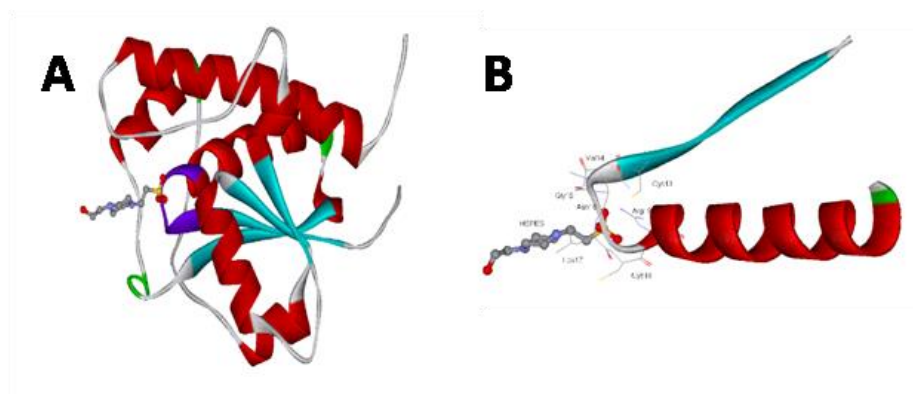


**Figure 5.** (A). Schematic diagram of Bovin heart PTPs (1DG9 )complexed with HEPES (B). Active site residues complexed with HEPES in 1DG9 (Template)

184

185 The fold energetic Dr-PTPs was calculated by program Prosa using template Bh-  
186 PTPs crystal structure. The comparison of energy was explored as shown by  
187 energy graph (Fig. 6).

188



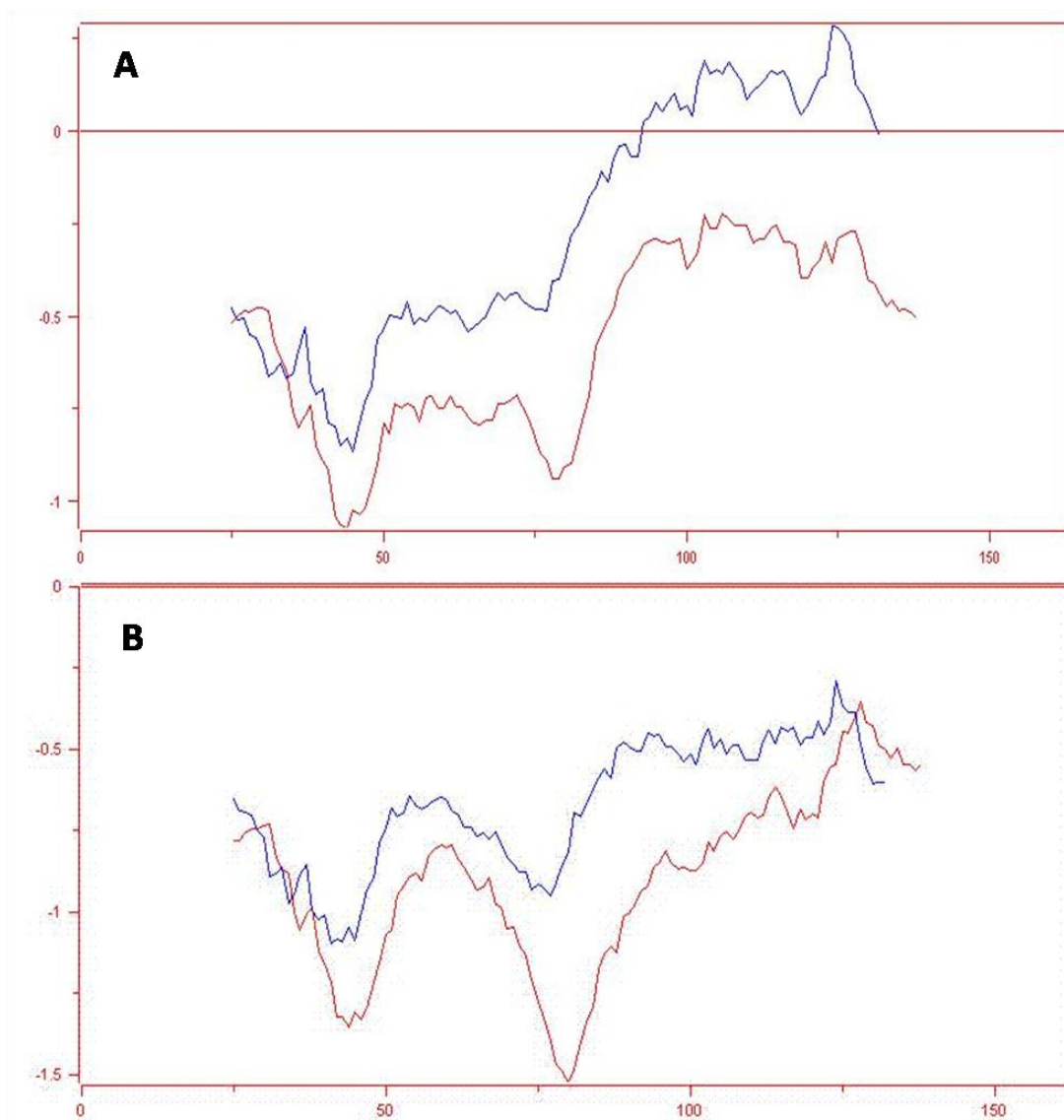


**Figure 6.** Comparison of PROSA II combined surface and pairing energy plots examined as a function of residue b/w template (blue) and the model (blue) for Bh-PTPs (A), 1DG9-PTPs, 1PNT-PTPs.

189

190 2.5. Active site and protein inhibitor interactions

191

192 The structural similarity of Dr-PTPs and Bh-PTPs and conformational  
193 resemblance of active site demonstrates the identity of catalytic mechanism. The  
194 catalytic reaction is triggered by the nucleophilic attack by Cys 3. The phosphate  
195 group at tyrosine group of the ligand or substrate bound at active site in  
196 orientation such that all the three oxygen atoms form hydrogen bonding with p-  
197 loop residues, making feasible the nucleophilic attack at phospho group by Cys3,  
198 Cys14, Cys16 and Cys18 where the Asp 129 works as proton donor resulting in

199 the formation of phosphoenzyme intermediate (17, 19). The hydrolytic cleavage  
200 of intermediate takesplace resulting in the formation of inorganic phosphate.  
201 The complexation of HEPES at active site of enzyme is stabilized by hydrophilic  
202 interactions like hydrogen bonding and hydrophobic electrostatic interactions  
203 and thus acts as a potent inhibitor. In Bh-PTPs (PDB: IDG9), the inhibitor HEPES  
204 is stabilized by forming seven hydrogen bonds with active site residues of  
205 enzyme. In similar fashion, nine hydrogen bonds were observed in Dr-PTPase. In  
206 case of Bh-PTPs, residues like Leu 13, Gly 14, Ile 16, Cys 17 and Arg 18 are  
207 involved in hydrogen bonding with inhibitor HEPES. Only three oxygens of  
208 HEPES involved in hydrogen bonding with active site residues of PTPs (Table 2).  
209 Residues like Val 14, Gly 15, Leu 17, Cys 18, Arg 19 participate in hydrogen  
210 bonding of Dr-PTPs (Target). Two nitrogen atoms and three oxygen atoms of  
211 HEPES (inhibitor) are involved in hydrogen bonding with active site residues of  
212 PTPase (Fig 7b).  
213

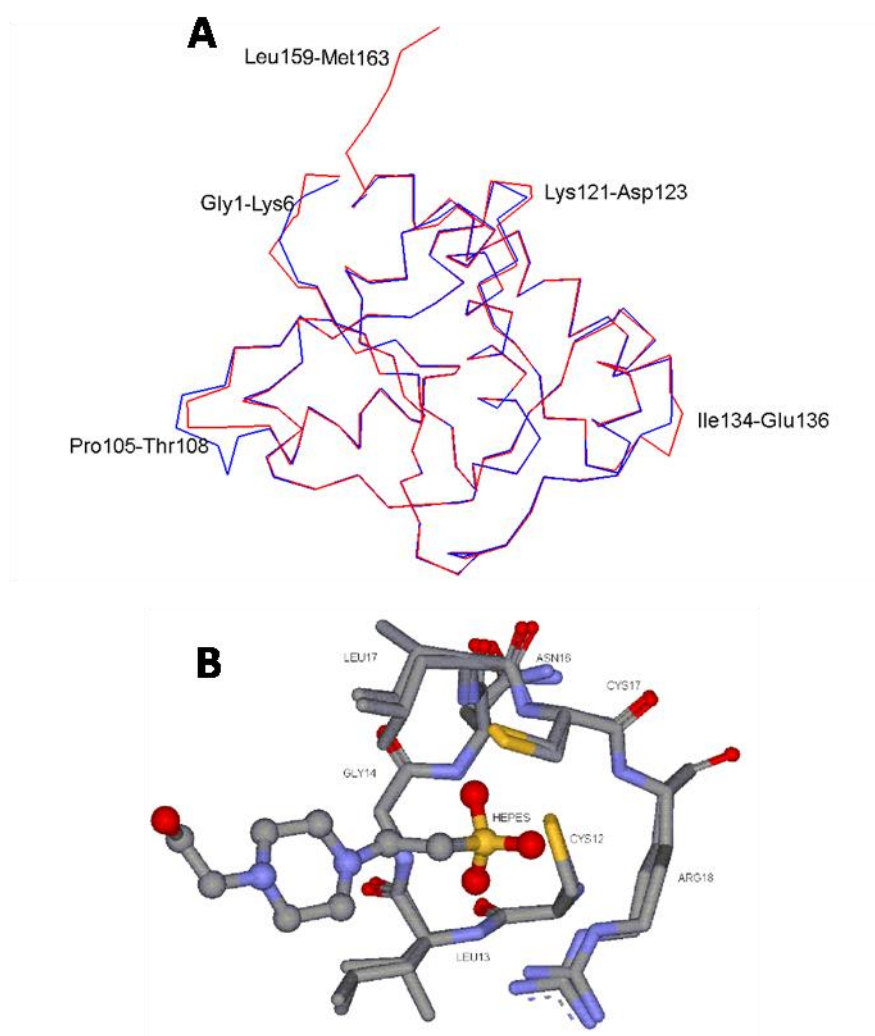


**Figure 7.** The active site is 100 % super imposed in template (Bh-PTPs) and Dr-PTPs. Active site is represented in sticks whereas inhibitor (HEPES) represents in ball and sticks style.

214

215 The stabilization of HEPES for complexation with Bh-PTPs is favored by  
216 hydrophobic interaction by residues Ile 16 and Tyr 131, while in Dr-PTPs, Leu 17,  
217 His 51 and Tyr 131 are involved in hydrophobic interactions.

218

219 **Table 2.** Ligand oxygen (HEPES)-Protein Nitrogen Bond length in PTPs complex

220

Bovine Heart PTPs Complex with HEPES			Drosophila PTPs Complex with HEPES		
1DG9	Amino acids	Distance (A <sup>0</sup> )	Model PTPs	Amino acids	Distance (A <sup>0</sup> )
EPE201:O1S	LEU13: N	3.17	EPE164:O1S	VA14: N	3.18
EPE201:O1S	GLY14: N	2.98	EPE164:O1S	GLY15: N	3.02
EPE201:O2S	ILE16: N	3.04	EPE164: C2	LEU17: N	3.06
EPE201:O2S	CYS17: N	2.88	EPE164:O2S	CYS18: N	2.88
EPE201:O1S	ARG 18: NH2	2.93	EPE164:O2S	ARG19: N	3.26
EPE201:O3S	ARG18: N	3.2	EPE164:O1S	ARG19: NH2	3.1
EPE201:O3S	ARG18: NE	2.94	EPE164:O3S	ARG19: NE	2.9
			EPE164: N1	EPE164: N4	2.99
			EPE164: N4	EPE164: N1	2.99

221

222

223 **Table 3.** Ligand oxygen (PO<sub>4</sub>)-Protein Nitrogen Bond length in PTPs complex

224

Bovine Heart PTPs Complex with PO <sub>4</sub>			Drosophila PTPs Complex with PO <sub>4</sub>		
1PNT	Aminoacids	Distance((A)	PPD10	Aminoacids	Distance(A)
PO4158:O3	LEU13:N	3.24	PO4164:O3	VAL14:N	3.24
PO4158:O3	GLY14:N	2.87	PO4164:O3	GLY15:N	2.91
PO4158:O2	ILE16:N	2.87	PO4164:O2	ASN16:N	3.28
PO4158:O2	CYS17:N	2.73	PO4164:O2	LEU17:N	2.9
PO4158:O3	ARG18:NH2	2.92	PO4164:O2	CYS18:N	2.74
PO4158:O4	ARG18:N	3.29	PO4164:O3	ARG19:NH2	3.06
PO4158:O4	ARG18:NE	2.78	PO4164:O4	ARG19:NE	2.94
			PO4164:O1	TYR131:OH	3.17
			PO4164:O3	PO4164:O4	2.51
			PO4164:O4	PO4164:O3	2.51

225

### 226 3. Materials and Methods

227

#### 228 3.1. Sequence analysis:

229 Sequence analysis of Dr-PTPs was obtained from SWISSPROT data base <sup>26</sup>. The  
230 sequence homology from the protein data bank was obtained from BLAST <sup>27,28</sup>,  
231 where modeller was used for target template alignment <sup>29</sup> for Dr-PTPs. The  
232 program Cluster was used for analysis of multiple sequences and adjustment of  
233 parameters made where necessary and finally, phylogenetic lineage was  
234 established with program phylip <sup>30,31</sup>.

235

236 3.2. Model building and refinement:

237

238 The three-dimensional model of Dr-PTPs was constructed using modeller (9V<sub>2</sub>)  
239 using Bh-PTPs crystal structure (PDB: 1DG9) as template model. The program  
240 was allowed to satisfy all dihedral angle, bond and spatial restraints and  
241 distances automatically as per default parameters. The input files consist of Dr-  
242 PTPs and Bh-PTPs aligned sequence. Several runs of calculations were  
243 performed to get more reliable and plausible model. The homology modeling  
244 was performed using standard parameters of calculations and known 3D  
245 structure models from protein data bank. The secondary structure elements of  
246 model were visualized using pymol and molmol <sup>16,31</sup> and other structural  
247 statistics was performed using psvs site  
248 (<https://montelionelab.chem.rpi.edu/PSVS>). The interaction of several ligands  
249 was analyzed using program Ligand Explorer  
250 (<http://users.sdsc.edu/~q2hang/ligand>) <sup>32</sup>.

251

252 3.3. Inhibitor modeling

253

254 The identification of hotspot residues, important for the target recognition and  
255 interaction was performed. The Dr-PTPs complexed with [N-(2-hydroxy ethyl)  
256 piperazine-N-2-ethanesulfonic acid sodium salt] (HEPES) was constructed using  
257 program modeller where the crystal structure 1DG9 was used as template. All  
258 these ligands known as potential inhibitors were models for the active sites for  
259 Dr-PTPs. The geometrical analysis, stereochemical analysis and all energies of  
260 bonds and dihedral restraints were analyzed. The homology models was  
261 subjected to program PROCHECK and ProSA for reliability of the model,  
262 secondary structure elements, backbone and energetic architecture and fold <sup>33-36</sup>.

263

#### 264 4. Conclusion

265 The sequence, secondary and tertiary structural similarities were studied in  
266 proteins Dr-PTPs and Bh-PTPs. The sequences of both proteins were found  
267 homologous for overall motifs and more especially for the active site motif  
268 represented by conserved residues C-(X)<sub>5</sub>-R. The comparative analysis of

269 sequences is evident on the fact that this strong signature (CXXXXXR) at active  
270 site is the characteristic of low Molecular weight phosphotyrosine protein  
271 phosphatases. It was found that residues in 10-27, 81-88, and 127-130 regions  
272 were highly conserved with low Molecular weight PTPs. The structure obtained  
273 for this novel sequence were found of reliable and valid based on analysis  
274 performed by various protein structure validation tools as shown by the  
275 ramachandran plot, PROCHECK, energy of the fold and comparative analysis  
276 with other template crystal structures. The complexation profile of Dr-PTPs was  
277 also established based on the potent inhibitor HEPES. The overall stabilization  
278 factors important for the inhibitor complexation were studied and compared  
279 with known literature. We found that strong conformational similarity of Dr-  
280 PTPs with other homologous PTPs may shares same types of inhibitors  
281 exclusively considered to inhibit low Molecular weight phosphotyrosine protein  
282 PTPS. All these structural details obtained from the model are important for  
283 scheming further specific inhibitors. It can be used as an additional probe to  
284 decipher the discrete biological role of the low Molecular weight  
285 phosphotyrosine PTPS family and to explore the potential use of these  
286 macromolecular species as therapeutic targets.

287

#### 288 **Data and Software Availability**

289 The data acquired in this manuscript is available for method validation and  
290 reproducibility of the results. We used softwares Clustalx<sup>30,37</sup>, Modeller<sup>29</sup>,  
291 Procheck<sup>33</sup> for make sequence alignments and modeling studies. The data  
292 obtained is available in supporting information or otherwise mentioned in the  
293 articles.

294

295 **Acknowledgment:** The project was financed by Lucian Blaga University of Sibiu  
296 and Hasso Plattner Foundation research grants LBUS-IRG-2021-07.

297

#### 298 **References**

- 299 (1) Kumar, A.; Rana, D.; Rana, R.; Bhatia, R. Protein Tyrosine Phosphatase  
300 (PTP1B): A Promising Drug Target Against Life-Threatening Ailments.  
301 *Current Molecular Pharmacology* **2020**, *13* (1), 17–30.  
302 <https://doi.org/10.2174/1874467212666190724150723>.
- 303 (2) Tonks, N. K. Protein Tyrosine Phosphatases: From Genes, to Function, to  
304 Disease. *Nature Reviews Molecular Cell Biology*. Nature Publishing Group  
305 November 2006, pp 833–846. <https://doi.org/10.1038/nrm2039>.
- 306 (3) Sa, N.; Rawat, R.; Thornburg, C.; Walker, K. D.; Roje, S. Identification and  
307 Characterization of the Missing Phosphatase on the Riboflavin  
308 Biosynthesis Pathway in *Arabidopsis Thaliana*. *The Plant Journal* **2016**, *88* (5),

- 309 705–716. <https://doi.org/10.1111/tpj.13291>.
- 310 (4) Niu, R. J.; Zheng, Q. C.; Zhang, H. X. Molecular Basis of the Recognition of  
311 FMN by a HAD Phosphatase TON\_0338. *Journal of Molecular Graphics and*  
312 *Modelling* **2016**, *69*, 17–25. <https://doi.org/10.1016/j.jmglm.2016.08.006>.
- 313 (5) Bull, H.; Murray, P. G.; Thomas, D.; Fraser, A. M.; Nelson, P. N. Acid  
314 Phosphatases. *Journal of Clinical Pathology - Molecular Pathology*. BMJ  
315 Publishing Group 2002, pp 65–72. <https://doi.org/10.1136/mp.55.2.65>.
- 316 (6) Logan, T. M.; Zhou, M. M.; Nettesheim, D. G.; Meadows, R. P.; Fesik, S. W.;  
317 Van Etten, R. L. Solution Structure of a Low Molecular Weight Protein  
318 Tyrosine Phosphatase. *Biochemistry* **1994**, *33* (37), 11087–11096.  
319 <https://doi.org/10.1021/bi00203a005>.
- 320 (7) Zhang, M.; Van Etten, R. L.; Stauffacher, C. V. Crystal Structure of Bovine  
321 Heart Phosphotyrosyl Phosphatase at 2.2-Å Resolution. *Biochemistry* **1994**,  
322 *33* (37), 11097–11105. <https://doi.org/10.1021/bi00203a006>.
- 323 (8) Zhang, Z. Y. Protein-Tyrosine Phosphatases: Biological Function,  
324 Structural Characteristics, and Mechanism of Catalysis. *Critical Reviews in*  
325 *Biochemistry and Molecular Biology*. Crit Rev Biochem Mol Biol 1998, pp 1–  
326 52. <https://doi.org/10.1080/10409239891204161>.
- 327 (9) Granjeiro, J. M.; Miranda, M. A.; Maia, M. D. G. S. T.; Ferreira, C. V.; Taga,  
328 E. M.; Aoyama, H.; Volpe, P. L. O. Effect of Homologous Series of N-Alkyl  
329 Sulfates and N-Alkyl Trimethylammonium Bromides on Low Molecular  
330 Mass Protein Tyrosine Phosphatase Activity. *Molecular and Cellular*  
331 *Biochemistry* **2004**, *265* (1–2), 133–140.  
332 <https://doi.org/10.1023/B:MCBI.0000044390.18530.39>.
- 333 (10) Evans, B.; Tishmack, P. A.; Pokalsky, C.; Zhang, M.; Van Etten, R. L. Site-  
334 Directed Mutagenesis, Kinetic, and Spectroscopic Studies of the P- Loop  
335 Residues in a Low Molecular Weight Protein Tyrosine Phosphatase.  
336 *Biochemistry* **1996**, *35* (42), 13609–13617. <https://doi.org/10.1021/bi9605651>.
- 337 (11) Tailor, P.; Gilman, J.; Williams, S.; Couture, C.; Mustelin, T. Regulation of  
338 the Low Molecular Weight Phosphotyrosine Phosphatase by  
339 Phosphorylation at Tyrosines 131 and 132. *Journal of Biological Chemistry*  
340 **1997**, *272* (9), 5371–5374. <https://doi.org/10.1074/jbc.272.9.5371>.
- 341 (12) Yuvaniyama, J.; Denu, J. M.; Dixon, J. E.; Saper, M. A. Crystal Structure of  
342 the Dual Specificity Protein Phosphatase VHR. *Science* **1996**, *272* (5266),  
343 1328–1331. <https://doi.org/10.1126/science.272.5266.1328>.
- 344 (13) Nam, H.-J.; Poy, F.; Krueger, N. X.; Saito, H.; Frederick, C. A. Crystal  
345 Structure of the Tandem Phosphatase Domains of RPTP LAR. *Cell* **1999**, *97*  
346 (4), 449–457. [https://doi.org/10.1016/S0092-8674\(00\)80755-2](https://doi.org/10.1016/S0092-8674(00)80755-2).
- 347 (14) Kennelly, P. J. Life among the Primitives: Protein O-Phosphatases in  
348 Prokaryotes. *Frontiers in Bioscience* **1999**, *4* (1–3), d372.

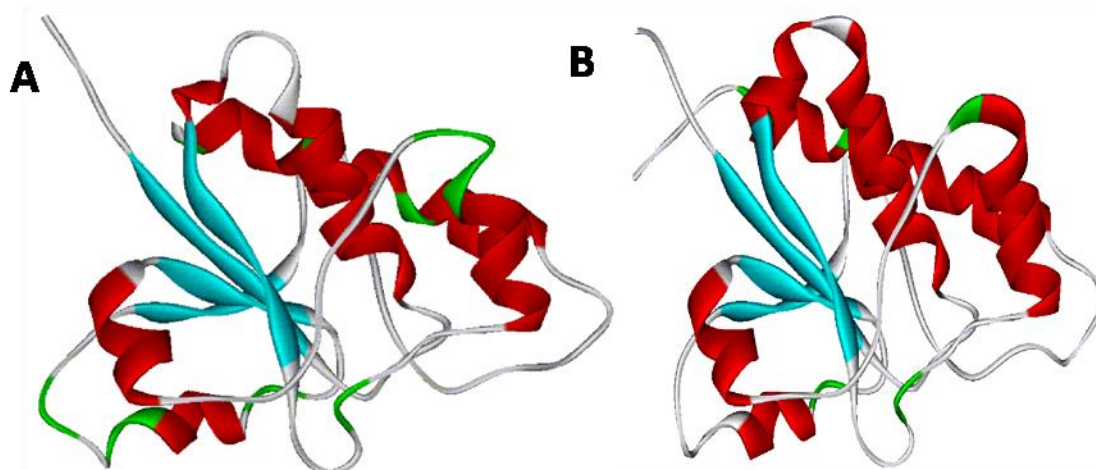
- 349 <https://doi.org/10.2741/kennelly>.
- 350 (15) Hoffmann, K. M. V.; Tonks, N. K.; Barford, D. The Crystal Structure of  
351 Domain 1 of Receptor Protein-Tyrosine Phosphatase  $\mu$ . *Journal of Biological*  
352 *Chemistry* **1997**, *272* (44), 27505–27508.  
353 <https://doi.org/10.1074/jbc.272.44.27505>.
- 354 (16) Glover, N. R.; Tracey, A. S. The Phosphatase Domains of LAR, CD45, and  
355 PTP1B: Structural Correlations with Peptide-Based Inhibitors 1 .  
356 *Biochemistry and Cell Biology* **2000**, *78* (1), 39–50. [https://doi.org/10.1139/o99-](https://doi.org/10.1139/o99-069)  
357 [069](https://doi.org/10.1139/o99-069).
- 358 (17) Zhang, M.; Stauffacher, C. V.; Lin, D.; Van Etten, R. L. Crystal Structure of  
359 a Human Low Molecular Weight Phosphotyrosyl Phosphatase. *Journal of*  
360 *Biological Chemistry* **1998**, *273* (34), 21714–21720.  
361 <https://doi.org/10.1074/jbc.273.34.21714>.
- 362 (18) Wang, S.; Taberero, L.; Zhang, M.; Harms, E.; Van Etten, R. L.;  
363 Stauffacher, C. V. Crystal Structures of a Low-Molecular Weight Protein  
364 Tyrosine Phosphatase from *Saccharomyces Cerevisiae* and Its Complex  
365 with the Substrate P-Nitrophenyl Phosphate. *Biochemistry* **2000**, *39* (8),  
366 1903–1914. <https://doi.org/10.1021/bi991348d>.
- 367 (19) Zhang, M.; Zhou, M.; Van Etten, R. L.; Stauffacher, C. V. Crystal Structure  
368 of Bovine Low Molecular Weight Phosphotyrosyl Phosphatase Complexed  
369 with the Transition State Analog Vanadate. *Biochemistry* **1997**, *36* (1), 15–23.  
370 <https://doi.org/10.1021/bi961804n>.
- 371 (20) Jia, Z.; Barford, D.; Flint, A. J.; Tonks, N. K. Structural Basis for  
372 Phosphotyrosine Peptide Recognition by Protein Tyrosine Phosphatase 1B.  
373 *Science* **1995**, *268* (5218), 1754–1758. <https://doi.org/10.1126/science.7540771>.
- 374 (21) Wo, Y. Y. P.; McCormack, A. L.; Shabanowitz, J.; Hunt, D. F.; Davis, J. P.;  
375 Mitchell, G. L.; Van Etten, R. L. Sequencing, Cloning, and Expression of  
376 Human Red Cell-Type Acid Phosphatase, a Cytoplasmic Phosphotyrosyl  
377 Protein Phosphatase. *Journal of Biological Chemistry* **1992**, *267* (15), 10856–  
378 10865. [https://doi.org/10.1016/s0021-9258\(19\)50097-7](https://doi.org/10.1016/s0021-9258(19)50097-7).
- 379 (22) Zhang, Z.; Harms, E.; Van Etten, R. L. Asp129 of Low Molecular Weight  
380 Protein Tyrosine Phosphatase Is Involved in Leaving Group Protonation.  
381 *Journal of Biological Chemistry* **1994**, *269* (42), 25947–25950.  
382 [https://doi.org/10.1016/s0021-9258\(18\)47139-6](https://doi.org/10.1016/s0021-9258(18)47139-6).
- 383 (23) Lau, K. H. W.; Farley, J. R.; Baylink, D. J. Phosphotyrosyl Protein  
384 Phosphatases. *Biochemical Journal*. 1989, pp 23–36.  
385 <https://doi.org/10.1042/bj2570023>.
- 386 (24) Wu, L.; Zhang, Z. Y. Probing the Function of Asp128 in the Low Molecular  
387 Weight Protein-Tyrosine Phosphatase-Catalyzed Reaction. A Pre-Steady-  
388 State and Steady-State Kinetic Investigation. *Biochemistry* **1996**, *35* (17),

- 389 5426–5434. <https://doi.org/10.1021/bi952885a>.
- 390 (25) Zhang, Z. Y.; Van Etten, R. L. Leaving Group Dependence and Proton  
391 Inventory Studies of the Phosphorylation of a Cytoplasmic Phosphotyrosyl  
392 Protein Phosphatase from Bovine Heart. *Biochemistry* **1991**, *30* (37), 8954–  
393 8959. <https://doi.org/10.1021/bi00101a006>.
- 394 (26) Bairoch, A.; Apweiler, R. The SWISS-PROT Protein Sequence Database and  
395 Its Supplement TrEMBL in 2000. *Nucleic Acids Research*. Oxford University  
396 Press January 1, 2000, pp 45–48. <https://doi.org/10.1093/nar/28.1.45>.
- 397 (27) Boratyn, G. M.; Camacho, C.; Cooper, P. S.; Coulouris, G.; Fong, A.; Ma, N.;  
398 Madden, T. L.; Matten, W. T.; McGinnis, S. D.; Merezuk, Y.; Raytselis, Y.;  
399 Sayers, E. W.; Tao, T.; Ye, J.; Zaretskaya, I. BLAST: A More Efficient Report  
400 with Usability Improvements. *Nucleic acids research* **2013**, *41* (Web Server  
401 issue). <https://doi.org/10.1093/nar/gkt282>.
- 402 (28) Morgulis, A.; Coulouris, G.; Raytselis, Y.; Madden, T. L.; Agarwala, R.;  
403 Schäffer, A. A. Database Indexing for Production MegaBLAST Searches. In  
404 *Bioinformatics*; Bioinformatics, 2008; Vol. 24, pp 1757–1764.  
405 <https://doi.org/10.1093/bioinformatics/btn322>.
- 406 (29) Eswar, N.; Webb, B.; Marti-Renom, M. A.; Madhusudhan, M. S.; Eramian,  
407 D.; Shen, M.; Pieper, U.; Sali, A. Comparative Protein Structure Modeling  
408 Using Modeller. *Current Protocols in Bioinformatics* **2006**, *15* (1), Unit.  
409 <https://doi.org/10.1002/0471250953.bi0506s15>.
- 410 (30) Wang, Y.; Wu, H.; Cai, Y. A Benchmark Study of Sequence Alignment  
411 Methods for Protein Clustering. *BMC Bioinformatics* **2018**, *19* (S19), 529.  
412 <https://doi.org/10.1186/s12859-018-2524-4>.
- 413 (31) Shimada, M. K.; Nishida, T. A Modification of the PHYLIP Program: A  
414 Solution for the Redundant Cluster Problem, and an Implementation of an  
415 Automatic Bootstrapping on Trees Inferred from Original Data. *Molecular*  
416 *Phylogenetics and Evolution* **2017**, *109*, 409–414.  
417 <https://doi.org/10.1016/j.ympev.2017.02.012>.
- 418 (32) Moreland, J. L.; Gramada, A.; Buzko, O. V.; Zhang, Q.; Bourne, P. E. The  
419 Molecular Biology Toolkit (MBT): A Modular Platform For Developing  
420 Molecular Visualization Applications. *BMC Bioinformatics* **2005**, *6* (1), 21.  
421 <https://doi.org/10.1186/1471-2105-6-21>.
- 422 (33) Laskowski, R. A.; MacArthur, M. W.; Moss, D. S.; Thornton, J. M.  
423 PROCHECK: A Program to Check the Stereochemical Quality of Protein  
424 Structures. *Journal of Applied Crystallography* **1993**, *26* (2), 283–291.  
425 <https://doi.org/10.1107/s0021889892009944>.
- 426 (34) Laskowski, R. A.; Rullmann, J. A. C.; MacArthur, M. W.; Kaptein, R.;  
427 Thornton, J. M. AQUA and PROCHECK-NMR: Programs for Checking the  
428 Quality of Protein Structures Solved by NMR. *Journal of Biomolecular NMR*



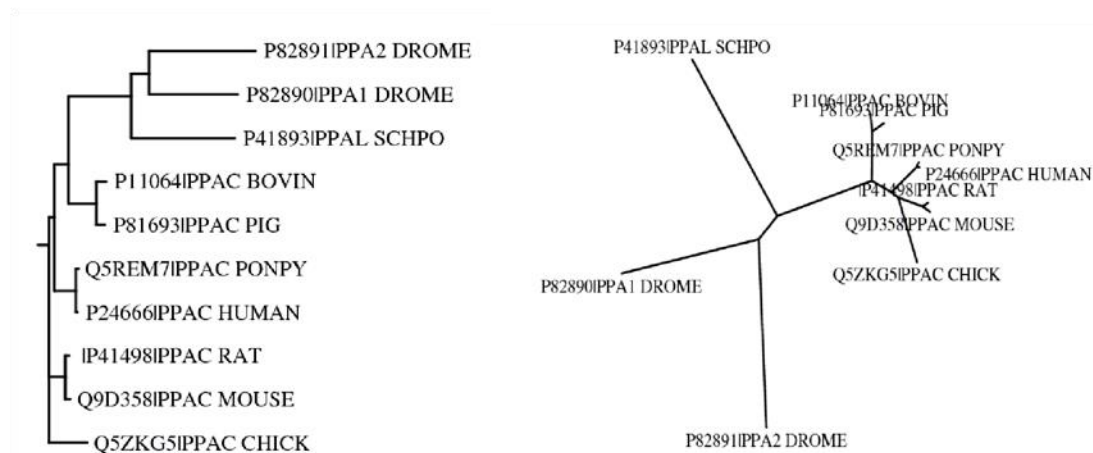
- 429           **1996**, 8 (4), 477–486. <https://doi.org/10.1007/BF00228148>.
- 430 (35) Furey, W.; Cowtan, K. D.; Zhang, K. Y. J.; Main, P.; Brunger, A. T.; Adams,  
431 P. D.; DeLano, W. L.; Gros, P.; Grosse-Kunstleve, R. W.; Jiang, J.-S.; Pannu,  
432 N. S.; Read, R. J.; Rice, L. M.; Simonson, T.; Tronrud, D. E.; Ten Eyck, L. F.;  
433 Lamzin, V. S.; Perrakis, A.; Wilson, K. S.; Laskowski, R. A.; MacArthur, M.  
434 W.; Thornton, J. M.; Kraulis, P. J.; Richardson, D. C.; Richardson, J. S.;  
435 Kabsch, W.; Sheldrick, G. M. Programs and Program Systems in Wide Use.  
436 In *International Tables for Crystallography*; International Union of  
437 Crystallography, 2006; pp 695–743.  
438 <https://doi.org/10.1107/97809553602060000724>.
- 439 (36) Wiederstein, M.; Sippl, M. J. ProSA-Web: Interactive Web Service for the  
440 Recognition of Errors in Three-Dimensional Structures of Proteins. *Nucleic*  
441 *Acids Research* **2007**, 35 (SUPPL.2), W407.  
442 <https://doi.org/10.1093/nar/gkm290>.
- 443 (37) Chenna, R.; Sugawara, H.; Koike, T.; Lopez, R.; Gibson, T. J.; Higgins, D.  
444 G.; Thompson, J. D. Multiple Sequence Alignment with the Clustal Series  
445 of Programs. *Nucleic Acids Research* **2003**, 31 (13), 3497–3500.  
446 <https://doi.org/10.1093/nar/gkg500>.
- 447





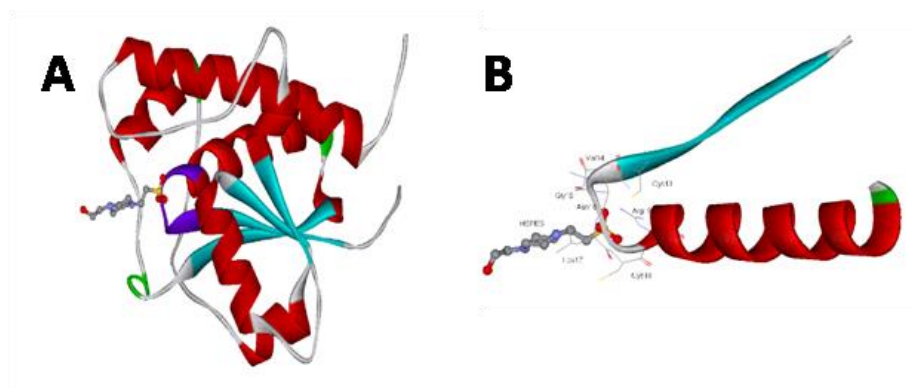
**Figure 3.** A complete Ribbon diagram of low molecular weight phosphotyrosine protein phosphatase. Showing  $\alpha/\beta$  Proteins,  $\alpha$  helix (Red),  $\beta$  Sheets (blue). (A) 1BVH(template), (B) Drosophila(target).

6  
7



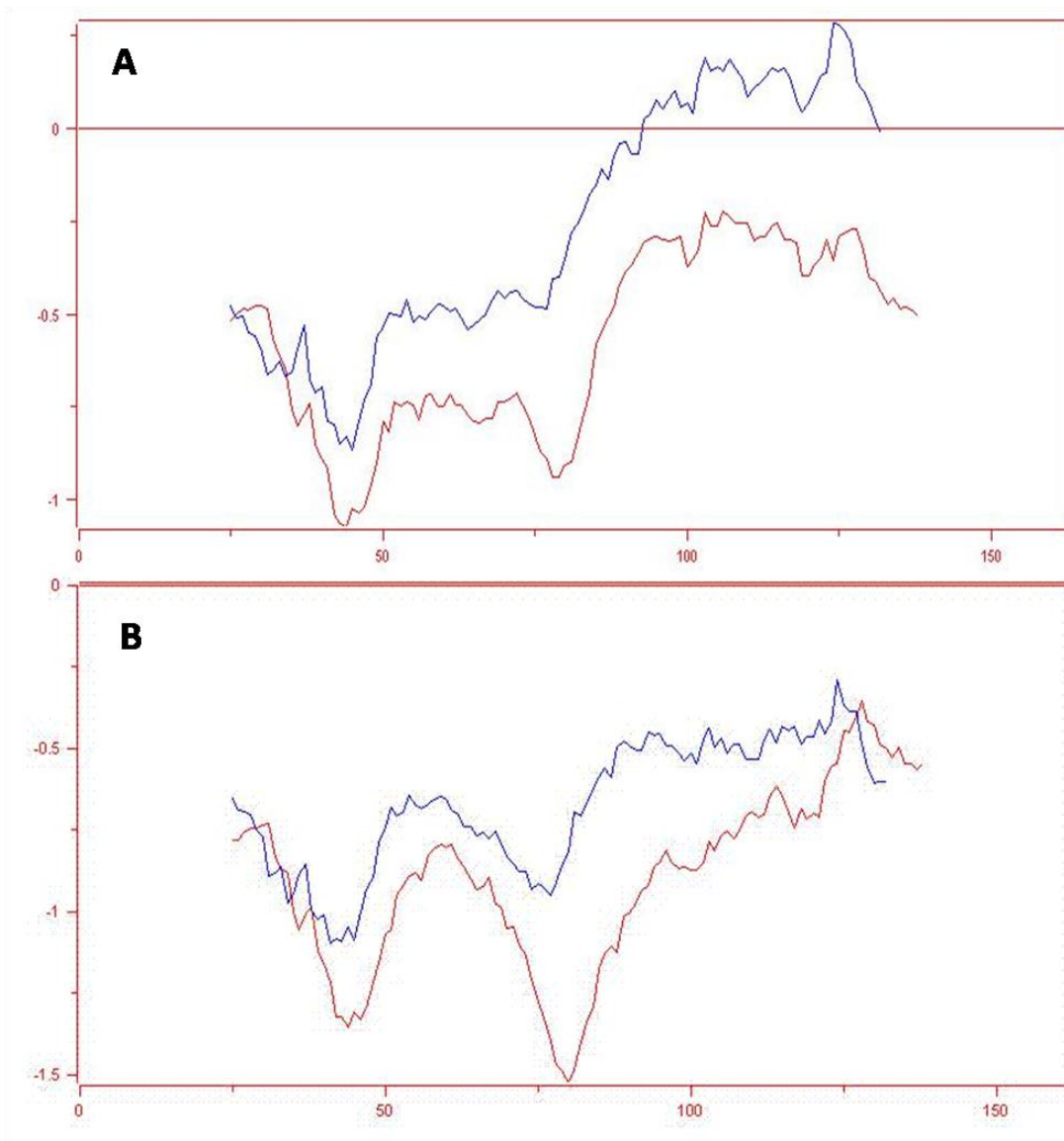
**Figure 4.** Dendrogram of PPA2 *Drosophila Melanogaster* and related proteins made by PHYLIP & depicts relationship among various forms of PPAC, PPAI, PPA2 genes. The first part of the code represents gene where as the second part of the code represents the source of protein.

8



**Figure 5.** (A). Schematic diagram of Bovin heart PTPs (1DG9) complexed with HEPES (B). Active site residues complexed with HEPES in 1DG9 (Template)

9



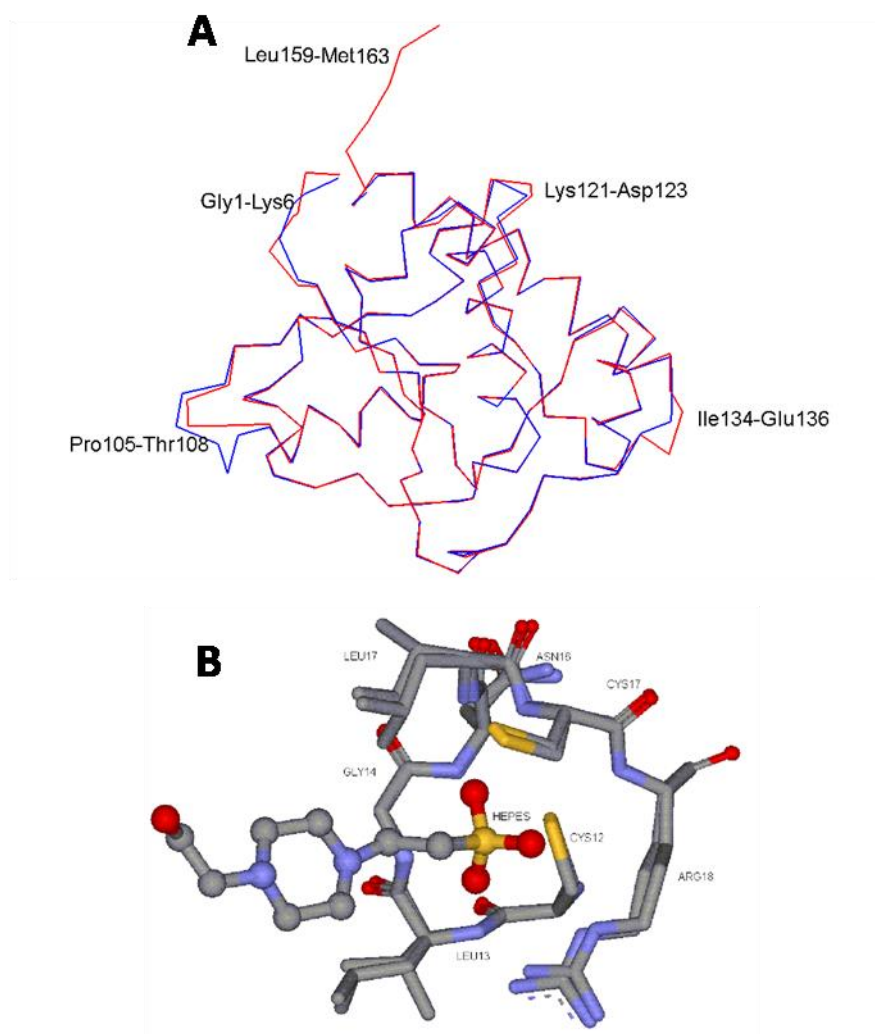


**Figure 7.** The active site is 100 % super imposed in template (Bh-PTPs) and Dr-PTPs. Active site is represented in sticks whereas inhibitor (HEPES) represents in ball and sticks style.